A Gaussian Process approach to multiple internal models in repetitive control

A Gaussian Process Approach to Multiple Internal Models in Repetitive Control

Noud Mooren*, Gert Witvoet *†, and Tom Oomen*‡
*Eindhoven University of Technology, Dept. of Mechanical Engineering, Control Systems Technology
Eindhoven, The Netherlands, email: n.f.m.mooren@tue.nl
† TNO, Optomechatronics Department, Delft, The Netherlands
‡ Delft Center for Systems and Control, Delft University of Technology, Delft, The Netherlands

***Abstract*—Disturbances that come from multiple originating domains, e.g., time, position, or commutation-angle domain, are often encountered in practice due to the increasing complexity of mechatronic systems. The aim of this paper is to present a generalized approach that enables asymptotic rejection of multi-dimensional disturbances which are periodic in the different originating domains, e.g., if speed changes, then spatially-periodic disturbances manifest themselves differently in the time domain. A multi-dimensional Gaussian process (GP) based internal model is employed in conjunction with a traditional repetitive control (RC) setting using non-equidistant observations, allowing to learn a multidimensional buffer for RC. A case study with a spatio-temporal disturbance confirms the benefit of this method.**

***Index Terms*—Repetitive control, Internal model control, Gaussian processes, Multi-dimensional disturbances**

I. Introduction

Asymptotic rejection of unknown disturbances plays an important role to improve the performance of high-precision mechatronic systems. A key enabler for asymptotic disturbance rejection is the internal model principle (IMP), which states that a model of the unknown disturbance must be incorporated in a stable feedback loop [1]. Commonly used examples of IMP include a Proportional Integral (PI) controller, where a model of a constant disturbance, i.e., an integrator, is included in the feedback loop [2], and an inverse notch filter to reject an oscillatory disturbance at a single known frequency. However, traditional feedback control performance is often not satisfactory in presence of varying disturbances. Several add-on type controllers for active disturbance rejection have been developed, including disturbance-observer-based control (DOBC) where a good model of the system is essential to estimate the exogenous unknown disturbance and consequently compensate for it, see, e.g., [3].

Engineered systems become increasingly complex, leading to disturbances that originate from different domains, e.g., time, position, or commutation angle [4], [5], referred to as multi-dimensional disturbances. Examples include an industrial printer where a rotating belt generates a disturbance that is periodic in the belt-position domain [6], where at the same time the print head generates a disturbance that is periodic in time due to its repeating motion [7]. Thermo-mechanical problems also appear, e.g., in wafer-stages with non-perfect commutations functions that induce spatial disturbances, while at the same time illumination of the wafer induces a thermal deformation [8], [9]. In view of these multi-dimensional disturbances, traditional internal models are not applicable as they contain only a single domain, whereas systematic integration of multiple internal models in different domains is required.

Disturbances that are periodic in the time domain can be asymptotically rejected using repetitive control (RC), where an internal disturbance model is learned in a time-domain memory loop of size is equal to the disturbance period time [10], [11]. RC is successfully applied to many industrial applications, including DC motors [12], printing systems [7] and hard-disk drives [13], [14]. To improve the flexibility of RC several extensions have been developed recently, e.g., multi-period disturbances in the time domain are compensated by using multiple RCs [15]–[17], and robustness for slight variations in the period-time is improved using multiple buffers in higher-order RC (HORC) [13], [18]. To cope with disturbances that are periodic in the position domain, where observations become non-equidistant, spatial RC is developed by exploiting spatial internal models [12]. Despite these recent improvements, existing RC approaches are not applicable when disturbances are periodic in multiple domains.

Although recent progress is made to enable asymptotic rejection of repeating disturbances, a unified framework that systematically integrates multiple domains is not yet available. Recent developments in RC utilize a Gaussian process (GP) based internal model to construct spatial [19] and temporal models [20]. These developments and the flexibility of GPs enables to systematically design multi-dimensional GP-based internal models for suppression of multi-dimensional disturbances in RC which is the aim of this paper. The main contribution of this paper is (C1) repetitive controller design for systematic integration of multi-dimensional periodic disturbances through a Gaussian-process-based buffer with a multi-dimensional additive periodic kernel, and (C2) a case study with a spatio-temporal disturbance.

This paper is outlined as follows, the problem is presented in Section II. In Section III, the GP-based internal model for RC is presented (C1), and in Section IV a case study with a spatio-temporal disturbance is shown (C2). Conclusions are given in Section V.

This research has received funding from the European Union H2020 program ECSEL-2016-1 under grant n. 737453 (I-MECH), and the ECSEL Joint Undertaking under grant agreement n. 101007311 (IMOCO4.E)

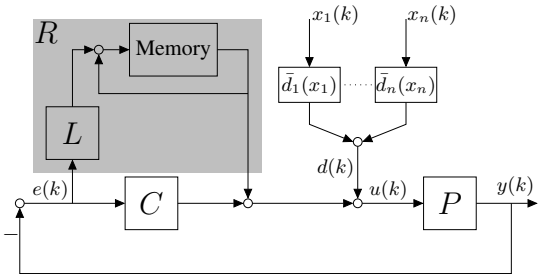

Fig. 1. Disturbance rejection problem with the n-dimensional disturbance $d(k)$ and the conventional repetitive controller structure R.

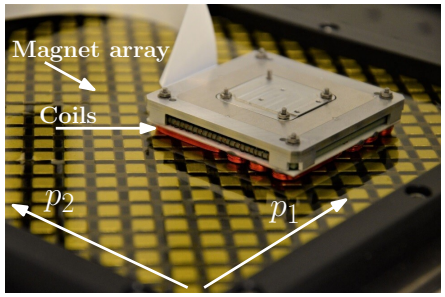

Fig. 2. Picture of a prototype magnetically levitated platform (maglev) on an array of permanent magnets used to carry a sample for Atomic Force Microscopy (AFM) [21]. If commutation is non-perfect then the magnets induce a disturbance as function of the positions x_1 and x_2.

II. Problem Formulation

A. Control setting

The control problem is depicted in Fig. 1, where P is a linear time-invariant (LTI) single-input single-output (SISO) discrete-time (DT) system, C is a stabilizing feedback controller, and R is a repetitive controller (RC) that is designed in the forthcoming sections. The aim of this paper is to design R such that the disturbance induced error given by

$$e_d(k) = -(1 + P(q)C(q))^{-1}P(q)d(k), \tag{1}$$

with q the unit time shift operator, i.e., $u(k-1) = q^{-1}u(k)$, is minimized in the presence of a multi-dimensional disturbance signal $d(k)$ that is in general non-periodic in time $k \in \mathbb{N}$ and defined in the following section.

B. Multi-dimensional disturbances in RC

The n-dimensional disturbance signal $d(k)$ in Fig. 1 is the summation of n signals $d_i(k)$ that are periodic in their respective domain x_i, e.g., position, time, or commutation angle, with $i \in \{1, 2, \dots n\}$. This is formally presented in the following definition, where the notation $\bar{(\cdot)}$ distinguishes functions from signals.

Definition 1 The discrete disturbance signal $d(k) \in \mathbb{R}$ at sample k is obtained by evaluating the continuous n-dimensional function $\bar{d}(\underline{x}(k)) : \mathbb{R}^n \to \mathbb{R}$ for any $\underline{x}(k) = \begin{bmatrix} x_1(k) & x_2(k) & \dots & x_n(k) \end{bmatrix}^\top \in \mathbb{R}^n$, i.e.,

$$d(k) = \bar{d}(\underline{x}(k)) = \sum_{i=1}^{n} \bar{d}_i(x_i(k)), \tag{2}$$

where the additive function $\bar{d}$ is a sum of n functions $\bar{d}_i(x_i) : \mathbb{R} \to \mathbb{R}$ that are periodic in the domain x_i, i.e., $\bar{d}_i(x_i) = \bar{d}_i(x_i + T_i)$ for all i where $T_i \in \mathbb{R}$ is the period that is known in advance. Furthermore, the signals $x_i(k)$ for $i = 1, 2, \dots n$ are known or can be measured noise-free, possibly uncorrelated in the general case and non-equidistantly sampled.

The signal $d_i(k) = \bar{d}_i(x_i(k))$ is periodic in time if $x_i(k)$ increases linearly, but in the general case it is assumed that d_i is non-periodic in time. The overall disturbance $d(k)$ is periodic in time if all d_i are periodic with time-domain periods t_i and there exists a least common multiple $t = \text{lcm}(t_1, t_2, \dots, t_n)$, otherwise $d(k)$ is non-periodic in time. This is further illustrated in the following motivating example.

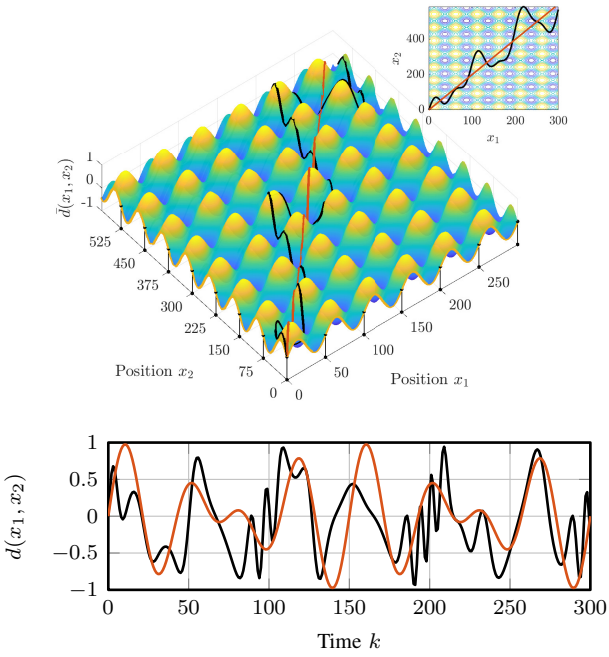

Fig. 3. Example 1: 2-dimensional disturbance mapping $\bar{d}(x_1, x_2)$ as function of x_1 and x_2, with periods $T_1 = 50$ and $T_2 = 75$ (top). The resulting disturbance $d(k)$ if $x_1 = 2x_2$ when $d(k)$ is periodic in time (—) and for varying x_1 and x_2 rendering $d(k)$ is non-periodic in time (—) (bottom).

Example 1 (2-dimensional disturbance in a maglev-stage) Consider the prototype magnetically levitated platform to carry a sample for atomic force microscopy in Fig. 2. Here, a 2-dimensional disturbance $d(x_1(k), x_2(k))$ acts on the platform if the commutation is non-perfect, where the position signals $x_1(k)$ and $x_2(k)$ are not correlated, see [21] for details. To replicate this setting, set $n = 2$ in (2) where x_1 and x_2 are the positions on the magnet array. The 2-dimensional disturbance function $\bar{d}(x_1, x_2)$ is replicated with $\bar{d}_1 = \frac{1}{2}\sin(2\pi\frac{x_1}{T_1})$ and $\bar{d}_2 = \frac{1}{2}\sin(2\pi\frac{x_2}{T_2})$ where $T_1 = 75$ and $T_2 = 50$ represent for example the magnet pitch, the resulting $\bar{d}(x_1, x_2)$ is depicted in Fig. 3. Consider the following cases.

i) If $x_1(k) = 2x_2(k)$ such that the platform moves diagonally and there is a static relation between x_1 and x_2, i.e., the matrix $\bar{X} = \begin{bmatrix} \bar{x}(1) & \bar{x}(2) & \dots & \bar{x}(k) \end{bmatrix} \in \mathbb{R}^{n \times k}$ is it

not full row rank, then $d(k)$ manifests periodic in time. The signal $d_1(x_1(k))$ has time-domain period $\frac{1}{2}T_1 = 37.5$ samples and $d_2(x_2(k))$ has $T_2 = 50$ samples, hence $\mathrm{lcm}(50, 37.5) = 150$ samples, see Fig. 3 in (—).

ii) If x_1 and x_2 vary continuously as in the top right in Fig. 3 in (—), then $\bar{X}$ is full row rank and there is no static relation. This renders $d(k)$ non-periodic in time (—).

Hence, if all signals x_i are uncorrelated the disturbance is non-periodic in time. Next, the limitations of traditional temporal buffers for the disturbances in Definition 1 are outlined.

C. Limitations of traditional RC

In traditional RC, a time-domain memory z^{-N} in a feedback loop is used to model the time-domain periodic disturbance. In the case of multi-dimensional disturbances, the main challenges that arise for RC are twofold, first, the memory loop must combine multiple domains, second, due to variations in $\underline{x}(k)$ the error data is non-equidistant in $\underline{x}(k)$. To compensate for the disturbance, the buffer must be a continuous function that is constructed from non-equidistant data and can be evaluated at any $\underline{x}(k) \in \mathbb{R}^n$. This implies that traditional memory loops, which rely on time-domain periodicity, cannot be used. Alternative RC approaches use non-equidistant data in the position-domain [22] by employing a Gaussian process (GP), but combining multiple uncorrelated domains in RC is not yet available.

D. Problem definition

The aim of this paper is to learn the multi-dimensional disturbance with an additive GP and suitable prior through a periodic kernel function in the underlying domains. By exploiting structure and periodicity in $\bar{d}$, the functions $\bar{d}_i$ are learned jointly from non-equidistant and non-periodic data.

III. Multi-dimensional repetitive control

A. Multi-dimensional buffer for RC

The multi-dimensional GP-based RC R is depicted in Fig. 4, where $\mathcal{GP}_B$ is the multi-dimensional GP-based buffer that replaces the time-domain memory z^{-N} from traditional RC, and L is a stable learning filter. GP regression is performed at every sample k to learn a model of the multi-dimensional disturbance function $\bar{d}(\underline{x})$, based on N data points that are non-equidistant in the domains $\underline{x}$. For compensation in RC, the GP-based model can be evaluated at any $\underline{x}(k) \in \mathbb{R}^n$.

The data for GP regression consists of the past N values of $y_d(k) \in \mathbb{R}$ and the corresponding $\underline{x}(k)$. These are collected in $Y(k) \in \mathbb{R}^N$ and $X(k) \in \mathbb{R}^{n \times N}$ respectively given by

$$Y(k) = \begin{bmatrix} y_d(k) & y_d(k-1) & \dots & y_d(k-N+1) \end{bmatrix}^\top, \quad (3a)$$

$$X(k) = \begin{bmatrix} \underline{x}(k)^\top & \underline{x}(k-1)^\top & \dots & \underline{x}(k-N+1)^\top \end{bmatrix}^\top. \quad (3b)$$

Define the n-dimensional training data set $\mathcal{D}_N(k) = (X, Y)$ containing N pairs $(y_d(k), \underline{x}(k))$.

The number of data points N may vary over time and is not correlated with the periodicity, which is the case in traditional memory loops. The periodicity in each of the underlying domains is embedded in the multi-dimensional prior as will be shown in the remainder of this section.

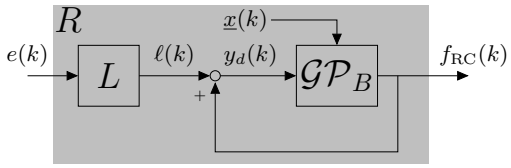

Fig. 4. Multi-dimensional repetitive controller R with learning filter L Gaussian-process-based buffer $\mathcal{GP}_B$.

B. $\mathcal{GP}$ regression for multi-dimensional disturbances

In this section, the multi-dimensional internal disturbance model of $\bar{d}$ is learned from the data $\mathcal{D}_N$ through Gaussian process regression. In GP regression is a distribution over functions is inferred from data and a suitable prior distribution [23], [24]. The n-dimensional and potentially non-equidistant data $\mathcal{D}_N$ is used to learn the posterior distribution over functions, that can be evaluated at any $\bar{x} \in \mathbb{R}^n$ for compensation in RC. Next, the prior knowledge and posterior distribution are defined to give an expression for the GP-RC output $f_{\mathrm{RC}}(k)$.

To define prior knowledge assuming that $\bar{d}(\underline{x})$ can be represented as a GP, i.e.,

$$\bar{d}(\underline{x}) \sim \mathcal{GP}(0, \kappa(\underline{x}, \underline{x}')), \quad (4)$$

where $\kappa(\underline{x}, \underline{x}')$ is an n-dimensional covariance function that describes the prior covariance between $\underline{x}$ and $\underline{x}'$, and the prior mean function is assumed to be zero a priori. Moreover, $\mathcal{D}_N$ contains noisy observations of the true disturbance, i.e., $Y(X) = \bar{d}(X) + \epsilon$ where $\epsilon \sim \mathcal{N}(0, \sigma_n^2 I_N)$ is zero-mean and follows an independent, identically distributed Gaussian distribution. To determine the posterior distribution at $\underline{x}_*(k) \in \mathbb{R}^n$ using $\mathcal{D}_N$ and prior knowledge (4) for compensation, assume a joint normal distribution between the test points $\underline{x}_*(k) \in \mathbb{R}^n$ and the training points $\mathcal{D}_N(X, Y)$

$$\begin{bmatrix} Y \\ \bar{d}_* \end{bmatrix} \sim \mathcal{N}\left(\begin{bmatrix} 0 \\ 0 \end{bmatrix}, \begin{bmatrix} K + \sigma_n^2 I_N & K_* \\ K_*^\top & K_{**} \end{bmatrix} \right), \quad (5)$$

where $K \in \mathbb{R}^{N \times N}$ is the covariance function $\kappa(X, X)$ evaluated at (X, X), and similar for $K_* = \kappa(X, X_*) \in \mathbb{R}^{N \times 1}$ and $K_{**} = \kappa(X_*, X_*) \in \mathbb{R}$. The posterior distribution at the test points $\underline{x}^*$ is given by $\mathrm{p}(\bar{d}_* | \mathcal{D}, X_*) = \mathcal{N}(\bar{d}, \Sigma)$ with

$$\bar{d}(X_*) = K_*^\top (K + \sigma_n^2 I_N)^{-1} Y, \quad (6a)$$

$$\Sigma(k) = K_{**} - K_*^\top (K + \sigma_n^2 I_N)^{-1} K_* \quad (6b)$$

the posterior mean and covariance respectively, see, e.g., [24]. For compensation in RC, the most likely sample from the posterior distribution (6), i.e., the posterior mean $\bar{d}(X_*)$, is used. The RC output for a test point $\underline{x}^*(k)$ is given by

$$f_{\mathrm{RC}}(k) = K_*^\top (K + \sigma_n^2 I_N)^{-1} Y(k). \quad (7)$$

The choice κ is essential to obtain an accurate model and be able to extrapolate beyond the given data points.

C. Multi-dimensional kernel selection

A suitable prior covariance function κ in (4) where periodicity in each of functions $\bar{d}_i$ is incorporated together with the additive structure in Definition 1 allows combine multiple

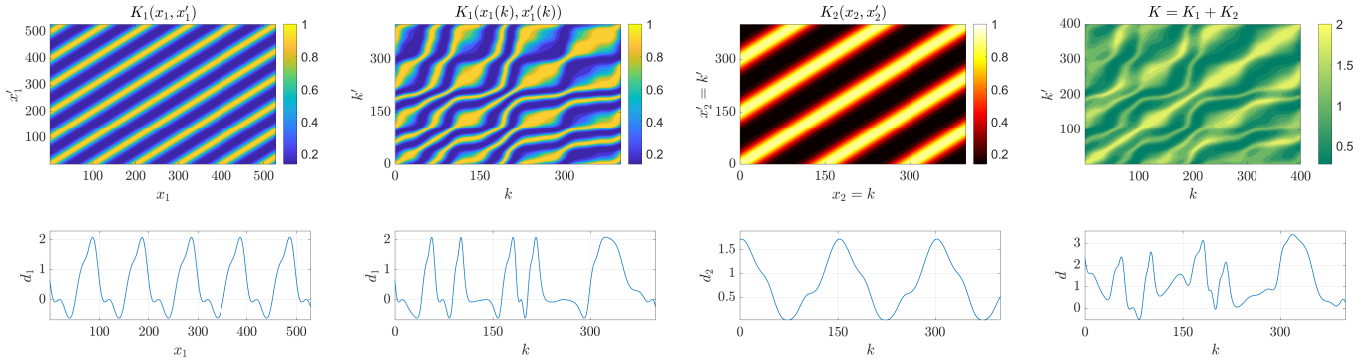

Fig. 5. Example 2 with a 2-dimensional spatio-temporal kernel $K(x_1, x_2) = K_1(x_1) + K_2(x_2)$ (fourth), that is the sum of two periodic kernels $K_1(x_1, x_1')$ (first) and $K_2(x_2, x_2')$ (third) with periods $T_1 = 100$ and $T_2 = 150$. Samples are taken from their corresponding prior distributions $\mathcal{N}(0, \kappa_i(X, X))$ that are periodic with T_1 and T_2 respectively. The kernel $K_1(x_1(k), x_1'(k))$ is also shown as function of k (second) where both the kernel and a random sample is non-periodic. Finally, the sum of K_1 and K_2 yields $K(\bar{x}(k))$ (fourth) that is non-periodic.

domains in a single GP-based buffer for RC. Assume that the functions $\bar{d}_i$ for $i = 1, 2, \ldots, n$ can be modeled as a GP, i.e., $\bar{d}_i(x_i) \sim \mathcal{GP}(0, \kappa_i(x_i, x_i'))$, where $\kappa_i(x_i, x_i')$ is the covariance function that specifies prior knowledge regarding $\bar{d}_i$. Since, each $\bar{d}_i$ is periodic and smooth, a periodic covariance function

$$\kappa_i(x_i, x_i') = \sigma_{f,i}^2 \exp\left(\frac{-2}{l_i^2} \cdot \sin^2\left(\frac{\pi |x_i - x_i'|}{T_i}\right)\right), \tag{8}$$

is used where l_i is the smoothness, T_i the period and $\sigma_{f,i}$ a gain, see, e.g., [24, Chapter 4]. Consequently, the multi-dimensional covariance function κ for $\bar{d}(\underline{x})$ in (4) is

$$\kappa(\underline{x}, \underline{x}') = \sum_{i=1}^{n} \kappa_i(x_i, x_i'), \tag{9}$$

which is an additive n-dimensional covariance function [25].

As a result, a sample taken from the prior distribution $\mathcal{N}(0, \kappa(X, X'))$ with covariance function (9) is smooth and can be decomposed in a sum of smooth and periodic functions in each of the underlying domains x_i as illustrated next.

Example 2 (Spatio-temporal kernel) Consider $n = 2$ in (9) with hyperparameters $T_1 = 100$, $T_2 = 150$, $l_1 = l_2 = 1$ and $\sigma_{f,1}^2 = \sigma_{f,2}^2 = 1$. The signal $x_1(k)$ is a position signal that varies over time and $x_2 = k$, i.e., a spatio-temporal setting. The kernel matrices $K_1(x_1, x_1')$, $K_2(k, k')$ and the sum $K(\underline{x}, \underline{x}') = K_1(x_1, x_1') + K_2(k, k')$ and samples drawn from the corresponding prior distributions $\mathcal{N}(0, K_i)$ are shown in Fig. 5. The following observations are made.

- The kernel matrix $K_1(x_1, x_1')$ with period $T_1 = 100$ is large for any pair (x_1, x_1') where $|x_1 - x_1'| \approx 100$ and is small elsewhere. This implies that x_1 and x_1' are correlated if i) they are close together (smoothness) or they are T_i samples apart (periodicity). A random sample from $\mathcal{N}(0, \kappa(X, X'))$ is shown below, which is indeed periodic and smooth similar to K_2 with period 150.
- The kernel $K_1(x_1(k), x_1'(k))$ and its samples are non-periodic in time. Plot two in Fig. 5 shows K_1 and its sample directly as a function of time k instead of $x_1(k)$, this yields a non-periodic kernel and non-periodic sample that depends on the specific variation of $x_1(k)$ over time.
- The 2-dimensional additive kernel $K(\underline{x}, \underline{x}')$ with $\underline{x} = \begin{bmatrix} x_1 & x_2 \end{bmatrix}^\top$ is non-periodic as a function of k in the general case. Samples taken from the corresponding prior distribution $\mathcal{N}(0, \kappa(X, X'))$ are the sum of a sample from the individual prior distributions in the time domain due to the additive kernel structure.

Example 2 shows that the n-dimensional kernel $K(\bar{x}(k))$ is non-periodic while the underlying kernels $K_1(x_1, x_1')$ and $K_2(x_1, x_1')$ are periodic in x_1 and x_2 respectively. This allows to integrate multiple domain with their periodicity, while perform GP regression with time-domain data. Also, note that the discrepancies between coils are averaged out with a periodic kernel. These differences can be taken into account with a locally periodic kernel, see, [26].

D. Design procedure for GP-based RC

Procedure 1 (Multi-dimensional RC design)

Given a model of the process sensitivity SP perform;

1) Design $L \approx (SP)^{-1}$ with $S = (1 + SP)^{-1}$ as a stable inverse as in [10], [11], e.g., using ZPETC [27].
2) Select $N \in \mathbb{N}$, determine n in Definition 1 by identifying the sources of the disturbance, and select the kernel hyperparameters in (9). As a guideline one can select N as the sum of the underlying periods, i.e, $N = \sum_{i=1}^{n} T_i$.
3) At each time step k:
   a) Add the new sample $(\underline{x}_i(k), y_d(k))$ to $\mathcal{D}_N$ and compute the RC output using (7).
   b) If $\mathcal{D}_N$ exceeds N, remove $(\underline{x}(k - N), y_d(k - N))$ from $\mathcal{D}_N$.

Conditions for closed-loop stability for the presented approach are equivalent to the results in [22] and omitted due to space restrictions. Moreover, there is a trade-off in the number of data points N used for GP regression, i.e., a better model can be obtained at the cost of increased computational complexity. Several approaches are available to reduce the computational complexity of GP regression, see, e.g., [22], [28].

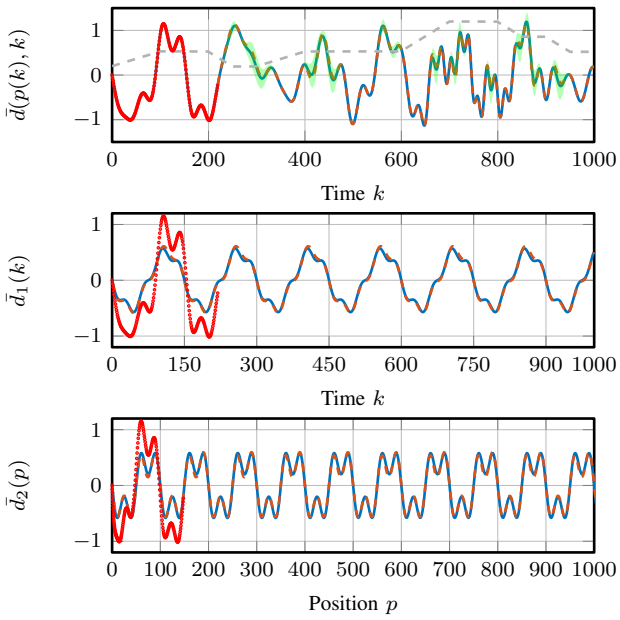

Fig. 6. Top plot: spatio-temporal disturbance $\bar{d}(p,k) = \bar{d}_1(k) + \bar{d}_2(p)$ that is non-periodic in time (—) from which observations (●) are used for GP regression yielding the posterior mean (- -) and variance ( ). The position signal p is given in (- -). Center plot: underlying temporally periodic disturbance component $\bar{d}_k$ (—) with period $T_1 = 150$ and the GP estimate (- -). Bottom plot: underlying spatially periodic disturbance component $\bar{d}_p$ (—) with period $T_2 = 100$ and the GP estimate (- -) as function of position.

Remark 1 If L is won-causal with n_l samples preview, then implement its causal part L_c as learning filter and replace $\underline{x}(k)$ by $\underline{x}(k - n_l)$ in (3b) to include preview.

Remark 2 If the smoothness in (8) is large, it may be redundant to use all data points for GP regression, i.e., two neighboring samples are highly correlated. As a measure for redundancy, the singular values of $(K + \sigma_n^2 I_N)$ can be used, i.e., if the new singular value is small for a newly data point it can be discarded from $\mathcal{D}_N$.

IV. Rejecting 2D spatio-temporal disturbances

The rejection of spatio-temporal disturbances through GPRC is shown in the following case study. These disturbances are encountered in, e.g., printing systems with a temporally periodic motion and at the same time a roller with varying angular velocity for paper transportation that induces a spatially periodic disturbance [6], [29]. A similar setting is considered in the following case study.

A. System and spatio-temporal disturbance

Consider the control setting in Fig. 1 with

$$P = \frac{0.05(z+1)}{z^2 - 1.98z + 1}, C = \frac{5.005(z+1)(z-0.81)}{(z+0.52)(z-0.03)},$$

the system and stabilizing feedback controller. A spatio-temporal disturbance as in Definition 1 is present for $n = 2$, where the spatial and temporal functions are

$$\bar{d}_1(k) = \tfrac{1}{2}\sin\left(\tfrac{2\pi}{T_1}k\right) + \tfrac{1}{10}\sin\left(4\tfrac{2\pi}{T_1}k\right)$$
$$\bar{d}_2(p) = \tfrac{1}{2}\sin\left(\tfrac{2\pi}{T_2}p\right) + \tfrac{3}{10}\sin\left(3\tfrac{2\pi}{T_2}p\right)$$

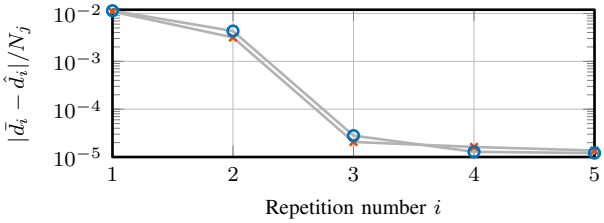

Fig. 7. The 2-norm of the estimation errors for $\bar{d}_1$ (×) and $\bar{d}_2$ (○) computed over the periods T_1 and T_2 respectively, normalized by the period length N_i in samples. An accurate estimate is obtained after $i = 2$ periods.

respectively, with periods $T_1 = 150$ and $T_2 = 100$ as show in the second and third plot in Fig. 6 in (—). The (roller) velocity of $p(k)$ varies over time, see (- -) in Fig. 6, rendering $d(k)$ non-periodic in time, see (—) in Fig. 6 (top plot) as in Example 1. Moreover, $d(k)$ is subject to additive zero-mean normally distributed white noise with variance $\sigma_n^2 = 10^{-6}$.

B. Multi-dimensional GPRC design

The L filter is designed with Procedure 1. All available data is used for GP regression such that N increases over time. Note that N is a design parameter, i.e., there is a trade-off between small N to reduce computation time and large N for estimation performance. The hyperparameters are chosen as $T_1 = 150$, $T_2 = 100$, $l_1 = l_2 = 1$, $\sigma_{f,1} = \sigma_{f,2} = 0.5$ and $\sigma_n^2 = 10^{-6}$. By increasing l, a less high-frequency RC output is obtained to improve robustness against model errors [20].

C. Estimation performance

First, the estimation performance of the GP without RC is investigated with a small number of noisy observations $N = 220$ for training. Consequently, predictions are made outside of the training data and compared with the true disturbance. The result is shown in Fig. 6, where (●) are the observations, (- -) the posterior mean, and 99.7% the confidence bound ( ).

An accurate estimate of the true disturbance, that is non-periodic in time, is obtained by estimating the underlying periodic functions (second an third plot) which is accurately extrapolated with periodic priors. Where the estimate deviates from the true disturbance the variance increases indicating that the estimate is less reliable.

D. GP-based RC results

Control performance is analyzed with the error in Fig. 8 without GP-RC (—) and with GP-RC (—). As a measure for convergence the 2-norm of the estimation error for $d_1(p)$ and $d_2(k)$ is computed for $i = 1, 2$ during the periods T_1 and T_2 respectively, see Fig. 7. The following observations are made:

- The non-periodic multi-dimensional disturbance is completely suppressed with GP-based RC in the first few samples, see Fig. 8. The bottom plot in Fig. 8 shows the moving mean of e on a log-scale confirming that GPRC reduces the error up to the contribution of the noise (—).
- The non-periodic disturbance is learned through the periodic functions in the time and position domain. The 2-norm of the estimation error for $\bar{d}_i$ is shown in Fig. 7 indicating that after $i = 2$ periods the estimation errors

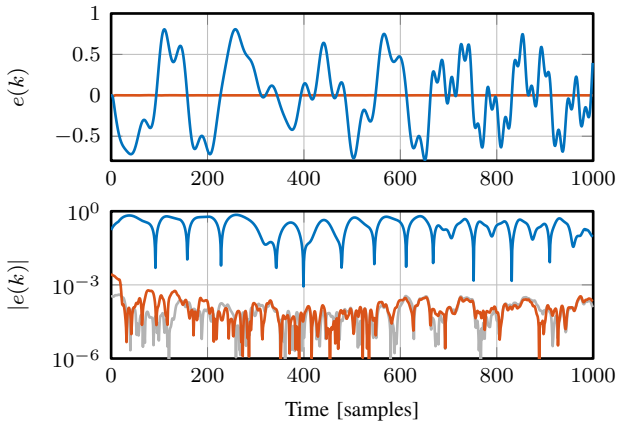

Fig. 8. Error with feedback control (—) and with GP-based RC (—) as function of time (top plot) and the absolute value of the error on a logarithmic scale (bottom plot). As a comparison the contribution of the noise to the error is given in (—) (bottom plot) as a lower-bound for achievable performance.

are converged. This implies that also with fewer data good control performance can be obtained.

To conclude, the considered GP-based multi-dimensional buffer for RC enables the rejection of multi-dimensional disturbances for arbitrary variations in $\underline{x}(k)$ over time.

V. Conclusion

The rejection of a multi-dimensional disturbance that is potentially non-periodic in time and periodic in multiple uncorrelated underlying domains, e.g., position, time, or commutation angle, is enabled through a multi-dimensional GP-based buffer in the traditional RC setting. Traditional disturbance models in RC cannot cope with the non-periodicity in the time-domain and integrating multiple domains requires new internal models for RC. In this approach, a new GP-based multi-dimensional internal disturbance model is generated by taking into account the underlying structure and periodicity in each of the domains through a multi-dimensional covariance function. Consequently, the GP-buffer is used for compensation. The approach is validated by means of a case study where a spatio-temporal disturbance is rejected for arbitrary position variations. Ongoing work focuses on utilizing the GP posterior variance as varying learning gain in RC.

References

[1] B. Francis and W. Wonham, "The internal model principle of control theory," *Automatica*, vol. 12, no. 5, pp. 457–465, 1976.

[2] D. Rivera, M. Morari, and S. Skogestad, "Internal model control: Pid controller design," *Industrial & engineering chemistry process design and development*, vol. 25, no. 1, pp. 252–265, 1986.

[3] S. Li, J. Yang, W. Chen, and X. Chen, *Disturbance observer-based control: methods and applications*. CRC press, 2014.

[4] D. J. Hoelzle and K. L. Barton, "On spatial iterative learning control via 2-d convolution: Stability analysis and computational efficiency," *IEEE Transactions on Control Systems Technology*, vol. 24, no. 4, pp. 1504–1512, 2016.

[5] N. Strijbosch, P. Tacx, E. Verschueren, and T. Oomen, "Commutation angle iterative learning control: Enhancing piezo-stepper actuator waveforms," *Auto*, vol. 12, no. 5, pp. 457–465, 1976.

[6] N. Mooren, G. Witvoet, I. Açan, J. Kooijman, and T. Oomen, "Suppressing position-dependent disturbances in repetitive control: With application to a substrate carrier system," in *2020 IEEE 16th International Workshop on Advanced Motion Control (AMC)*. IEEE, 2020, pp. 331–336.

[7] L. Blanken, T. Hazelaar, S. Koekebakker, and T. Oomen, "Multivariable repetitive control design framework applied to flatbed printing with continuous media flow," in *2017 IEEE 56th Annual Conference on Decision and Control (CDC)*. IEEE, 2017, pp. 4727–4732.

[8] D. Veldman, R. Fey, H. Zwart, M. van de Wal, J. van den Boom, and H. Nijmeijer, "Optimal thermal actuation for mitigation of heat-induced wafer deformation," *IEEE Transactions on Control Systems Technology*, 2019.

[9] E. Evers, N. van Tuijl, R. Lamers, and T. Oomen, "Identifying thermal dynamics for precision motion control," *IFAC-PapersOnLine*, vol. 52, no. 15, pp. 73–78, 2019.

[10] G. Goodwin and K. Sin, *Adaptive filtering prediction and control*. Courier Corporation, 2014.

[11] S. Hara, Y. Yamamoto, T. Omata, and M. Nakano, "Repetitive control system: A new type servo system for periodic exogenous signals," *IEEE Transactions on Automatic Control*, vol. 33, no. 7, pp. 659–668, 1988.

[12] X. Huo, M. Wang, K. Liu, and X. Tong, "Attenuation of position-dependent periodic disturbance for rotary machines by improved spatial repetitive control with frequency alignment," *IEEE/ASME Transactions on Mechatronics*, pp. 1–1, 2019.

[13] M. Steinbuch, S. Weiland, and T. Singh, "Design of noise and period-time robust high-order repetitive control, with application to optical storage," *Automatica*, vol. 43, no. 12, pp. 2086–2095, 2007.

[14] H. Fujimoto, "RRO compensation of hard disk drives with multirate repetitive perfect tracking control," *IEEE Transactions on Industrial Electronics*, vol. 56, no. 10, pp. 3825–3831, 2009.

[15] K. Zhou, D. Wang, B. Zhang, Y. Wang, J. Ferreira, and S. de Haan, "Dual-mode structure digital repetitive control," *Automatica*, vol. 43, no. 3, pp. 546–554, 2007.

[16] W. Chang, I. Suh, and J. Oh, "Synthesis and analysis of digital multiple repetitive control systems," in *Proceedings of the 1998 American Control Conference. ACC*, vol. 5. IEEE, 1998, pp. 2687–2691.

[17] L. Blanken, P. Bevers, S. Koekebakker, and T. Oomen, "Sequential multiperiod repetitive control design with application to industrial wide-format printing," *IEEE/ASME Transactions on Mechatronics*, vol. 25, no. 2, pp. 770–778, 2020.

[18] G. Pipeleers, B. Demeulenaere, J. de Schutter, and J. Swevers, "Robust high-order repetitive control: optimal performance trade-offs," *Automatica*, vol. 44, no. 10, pp. 2628–2634, 2008.

[19] N. Mooren, G. Witvoet, and T. Oomen, "Gaussian process repetitive control for suppressing spatial disturbances," in *IFAC 21st Triennial World Congress*. IEEE, 2020.

[20] ——, "Gaussian process repetitive control: Beyond periodic internal models through kernels," *submitted*.

[21] L. Kramer, T. van den Dool, and G. Witvoet, "Demonstrator for nano-precision multi-agent maglev positioning platform for high throughput metrology," *IFAC-PapersOnLine*, vol. 52, no. 15, pp. 471–476, 2019.

[22] N. Mooren, G. Witvoet, and T. Oomen, "Gaussian process repetitive control with application to an industrial substrate carrier systems with spatial disturbances," *submitted*.

[23] K. Murphy, *Machine learning: a probabilistic perspective*. MIT press, 2012.

[24] C. Williams and C. E. Rasmussen, *Gaussian processes for machine learning*. MIT press Cambridge, MA, 2006, vol. 2, no. 3.

[25] N. Durrande, D. Ginsbourger, and O. Roustant, "Additive kernels for Gaussian process modeling," *arXiv preprint*, 2011.

[26] D. Duvenaud, "Automatic model construction with gaussian processes," Ph.D. dissertation, University of Cambridge, 2014.

[27] M. Tomizuka, "Zero phase error tracking algorithm for digital control," *Journal of Dynamic Systems, Measurement, and Control*, vol. 109, no. 1, pp. 65–68, 1987.

[28] E. Snelson and Z. Ghahramani, "Sparse Gaussian processes using pseudo-inputs," in *Advances in neural information processing systems*, 2006, pp. 1257–1264.

[29] L. Blanken, S. Koekebakker, and T. Oomen, "Multivariable repetitive control: Decentralized designs with application to continuous media flow printing," *IEEE/ASME Transactions on Mechatronics*, 2020.